

## Elucidating the Thermal, Chemical, and Mechanical Mechanisms of Ultraviolet Ablation in Poly(methyl methacrylate) via Molecular Dynamics Simulations

PATRICK F. CONFORTI, MANISH PRASAD, AND  
BARBARA J. GARRISON\*

*Department of Chemistry, 104 Chemistry Building, Penn State University,  
University Park, Pennsylvania 16802*

RECEIVED ON DECEMBER 17, 2007

Ⓜ This paper contains enhanced objects available on the Internet at <http://pubs.acs.org/acr>.

### CON SPECTUS

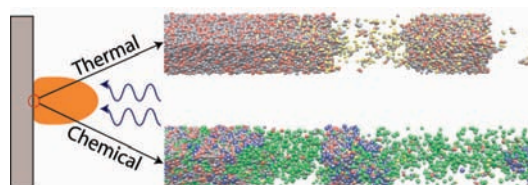
**L**aser ablation harnesses photon energy to remove material from a surface. Although applications such as laser-assisted in situ keratomileusis (LASIK) surgery, lithography, and nanoscale device fabrication take advantage of this process, a better understanding the underlying mechanism of ablation in polymeric materials remains much sought after.

Molecular simulation is a particularly attractive technique to study the basic aspects of ablation because it allows control over specific process parameters and enables observation of microscopic mechanistic details. This Account describes a hybrid molecular dynamics–Monte Carlo technique to simulate laser ablation in poly(methyl methacrylate) (PMMA). It also discusses the impact of thermal and chemical excitation on the ensuing ejection processes.

We used molecular dynamics simulation to study the molecular interactions in a coarse-grained PMMA substrate following photon absorption. To ascertain the role of chemistry in initiating ablation, we embedded a Monte Carlo protocol within the simulation framework. These calculations permit chemical reactions to occur probabilistically during the molecular dynamics calculation using predetermined reaction pathways and Arrhenius rates. With this hybrid scheme, we can examine thermal and chemical pathways of decomposition separately.

In the simulations, we observed distinct mechanisms of ablation for each type of photoexcitation pathway. Ablation via thermal processes is governed by a critical number of bond breaks following the deposition of energy. For the case in which an absorbed photon directly causes a bond scission, ablation occurs following the rapid chemical decomposition of material. A detailed analysis of the processes shows that a critical energy for ablation can describe this complex series of events. The simulations show a decrease in the critical energy with a greater amount of photochemistry. Additionally, the simulations demonstrate the effects of the energy deposition rate on the ejection mechanism. When the energy is deposited rapidly, not allowing for mechanical relaxation of the sample, the formation of a pressure wave and subsequent tensile wave dominates the ejection process.

This study provides insight into the influence of thermal, chemical, and mechanical processes in PMMA and facilitates greater understanding of the complex nature of polymer ablation. These simulations complement experiments that have used chemical design to harness the photochemical properties of materials to enhance laser ablation. We successfully fit the results of the simulations to established analytical models of both photothermal and photochemical ablation and demonstrate their relevance. Although the simulations are for PMMA, the mechanistic concepts are applicable to a large range of systems and provide a conceptual foundation for interpretation of experimental data.



## Introduction

Laser ablation is the massive removal of material that results from photon absorption. The process is used in a wide range of applications such as nanolithography and fabrication of organic light-emitting diodes (OLEDs).<sup>1–3</sup> The development of applications, however, is mostly decoupled from the basic processes occurring in the substrate. In polymeric materials, delineating the underlying cause of ablation remains a daunting task. The difficulties stem from the complex electronic and vibrational effects, which could result from photon absorption, as well as the convoluted interplay between the energy deposition and the mechanical, chemical, and structural properties of polymers. In order to untangle these complexities, simulations are presented in this Account that elucidate various mechanisms and provide insight into the ablation process.

In the literature, the most prevalent discussion focuses on the influence of two main mechanisms in causing ablation.<sup>4–7</sup> In one mechanism (photothermal), the photon absorption is followed by rapid thermalization and ablation occurs due to the explosive vaporization of the substrate.<sup>6,7</sup> In the other mechanism (photochemical), a molecule dissociates after excitation to an unstable electronic state and ablation takes place after the material decomposes.<sup>7–9</sup> Of course, these two mechanisms are the two idealized limits of the process occurring after excitation as they both undoubtedly contribute to material removal within one experiment. Indeed, various research groups have interpreted different photothermal and photochemical mechanisms as the origin of ablation for similar experiments.<sup>5,10–16</sup>

Though the terms “photothermal” and “photochemical” are used to describe ablation, a microscopic description of the processes involved in each mechanism is lacking. In experiment, clarifying such details is complicated by the fact that the litany of experimental conditions and material properties (such as laser wavelength, fluence, pulse duration, and absorption characteristics) each can influence an assortment of different molecular events.<sup>5–7,9,17–21</sup> For example, a variation in the laser wavelength causes significant changes in excitation and decomposition at the molecular level.<sup>13,16,17,22,23</sup> When ultraviolet (UV) and visible wavelengths are used, the energy available per photon is able to directly cause bond cleavages or themally breakdown molecules. When infrared (IR) wavelengths are used, thermal decomposition of molecules may take place.<sup>23–25</sup> When other conditions such as the laser fluence and absorption characteristics are varied, the effects can range from local perturbation of molecules to mesoscopic ejection.<sup>9,19,26,27</sup> These examples illustrate that a consistent

approach is needed to individually examine the impact of each aspect on the mechanisms of ablation.

An ideal technique for observing the effects of microscopic events in ablation is molecular dynamics (MD) simulation. MD simulations provide environments in which specific conditions such as fluence, wavelength, pulse width, and even chemistry can be incorporated and tested separately to observe their effects. By specifying interaction potentials and integrating the classical equations of motion, the trajectories of particles are calculated and various system properties such as energy, temperature, and pressure are stored at time intervals.<sup>28</sup> MD has successfully been utilized to describe the process of ablation from the microscopic atomic excitations to the mesoscopic ejection of material.<sup>29–33</sup> For instance, simulations provided a detailed description of ablation of a molecular solid with the appearance of clusters of substrate among the ejecta.<sup>34</sup> Additionally, photochemistry was included in simulations of chlorobenzene, and the energetics of the system were shown to play an important role in the ejection mechanism.<sup>35,36</sup>

This Account reports on the mechanisms of ablation in a poly(methyl methacrylate) system using an integrated approach to classically treat the photoexcitation and decomposition process. A method is described that permits widespread reactions to occur probabilistically during a MD simulation. Both photothermal and photochemical processes are studied, and their effects on the conditions necessary to achieve ablation are detailed. Connections between the simulations, analytical models, and experiment are illustrated.

## The Simulation Model

The nature of the material–light interaction in polymeric systems leading to ablation is extremely intricate, and no single simulation technique can appropriately capture the length and time scale involved. The process involves electronic or vibrational excitation, energy transfer, material decomposition, chemical reactions, and pressure fluctuations, as well as a dependence on the material properties, which includes chemical composition and molecular weight. While MD simulation cannot include all of these effects, it provides the most reasonable solution to observing how microscopic behavior can influence the ejection process on an experimentally relevant time scale.

The novel strategy that we have developed incorporates activated chemical reactions within a MD simulation without using complicated and computationally intensive potential functions.<sup>36,37</sup> This hybrid Monte Carlo (MC)–MD protocol is presented as a flowchart in Figure 1. The trajectories of the particles in the system are determined using the classical

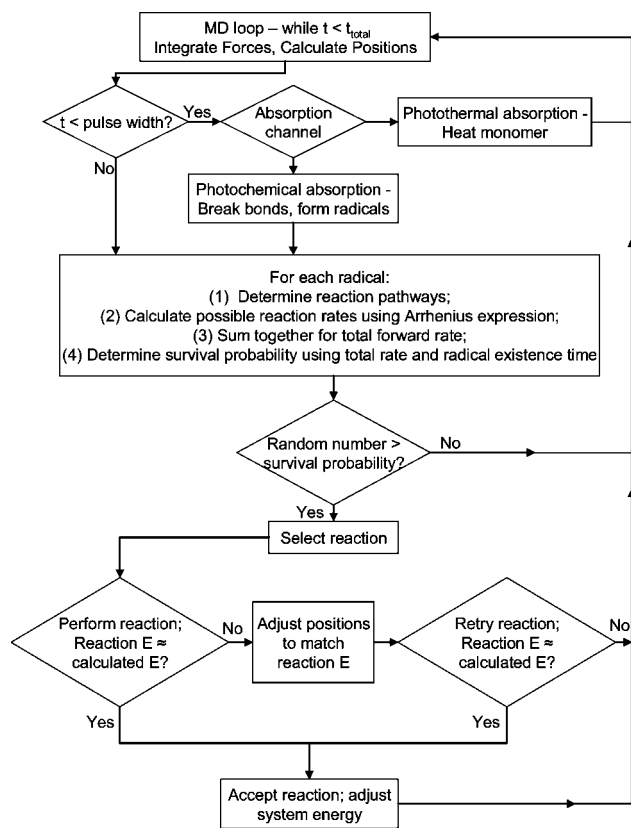


**FIGURE 1.** The flowchart for the Monte Carlo protocol, which includes chemical reactions during the MD simulations, where  $t$  is the simulation time and  $E$  is energy.

equations of motion. During the calculation, photons are absorbed by the substrate either thermally or photochemically when the simulation time is less than the laser pulse width. For photothermal absorption, we assume very rapid thermalization of the photon, and the energy heats a monomer unit around the absorption center. In photochemical absorption, we assume that a high-energy photon excites a molecule into a repulsive state and a covalent bond is broken forming two radical species. The quantum yield for this particular absorption channel is unity. If the photon does not have sufficient energy to break a covalent bond, photothermal absorption occurs. Radicals are tagged and attempt to react during the simulation. For each radical, there is a predetermined set of reaction pathways that it can traverse based on known mechanisms. At each time step, the Arrhenius reaction rates are calculated using activation energies and the local temperature for all possible pathways. The survival probability is then calculated using the total forward reaction rate (the sum of all the possible reactions rates) and the radical existence time. A random number is chosen, and if the number is less than the survival probability, the radical remains unchanged and continues to the next time step; else a reaction is attempted. If a reaction is attempted, another random

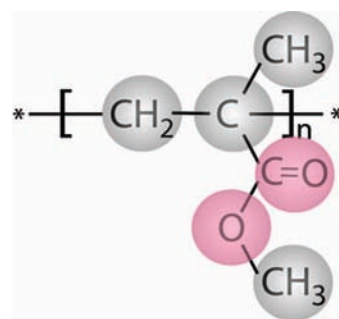


**FIGURE 2.** The chemical structure of a monomer unit of PMMA with the corresponding coarse-grained representation superimposed over it. The main chain C–CH<sub>2</sub> bond and side chain C–CO bonds are directly cleaved in the photochemical simulations.

number selects a reaction pathway based on the relative weight of each reaction rate. The reaction is performed by changing the reactants to product species and measuring the reaction energy. If the energy matches the experimental chemical reaction energy, the reaction is accepted, and the energy of the system is adjusted accordingly with the enthalpy. If the energy does not match, a steepest descent algorithm is used to reorganize and optimize the reactant state positions in order for the calculated energy to match the desired energy after the reaction is performed. If the optimization attains the experimental energy with minimal changes, the reaction is accepted; else the reaction is rejected. It is important to note that this model does not predict chemistry but includes the effects of chemistry in the ablation simulations. A detailed account of this procedure is given in ref 37.

In designing a model system to study the thermal and photochemical processes, we chose poly(methyl methacrylate), or PMMA, as a substrate. PMMA was chosen due to the wealth of experimental data available on laser interactions with PMMA along a wide range of experimental conditions, and moreover, PMMA exhibits significant photochemistry and diversity among the photoproducts.<sup>5,9,10,13,14,17,22,38</sup> Rather than an atomistic depiction of a PMMA molecule, the simulations use coarse-graining where the functional groups C, CH<sub>2</sub>, CH<sub>3</sub>, O, and C=O are each represented by a single united atom, see Figure 2. The use of united atoms eliminates the expensive C–H and C=O bond vibrations while retaining the necessary chemical information needed in the reaction scheme. The products that form following photoexcitation are well-documented in the literature.<sup>10,13,17</sup> A representative set of reactions is used in the simulations that includes gas and small molecule formation such as carbon monoxide, carbon dioxide, methane, methanol, methyl formate, and MMA monomer. Double-bonded carbons also are able to form from two adjacent bonded radicals. The activation and reaction

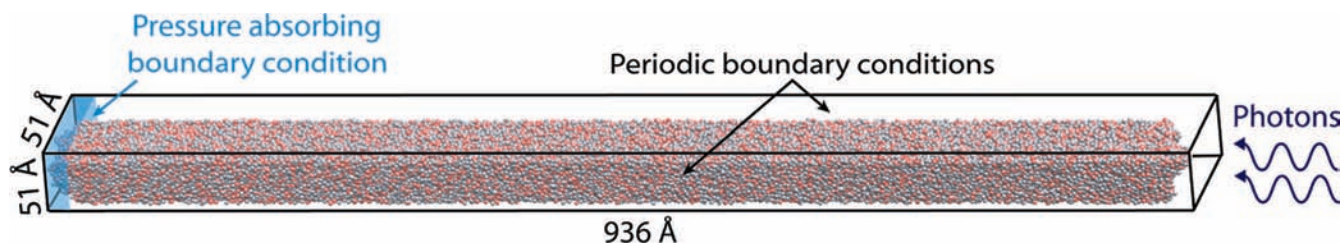


**FIGURE 3.** The computational setup for the MD simulations. Periodic boundary conditions are used on two sides of the cell simulating the center of the laser. A pressure-absorbing boundary condition is used on the bottom of the cell to represent an infinite solid.

energies for each species have been determined from electronic structure calculations.<sup>39</sup> By including a multitude of reaction products, we can extend our discussion of photochemical effects to aid in the understanding of ablation mechanisms of other substrates where similar processes may occur. For example, the exothermic decomposition of a triazene polymer into elemental nitrogen following laser irradiation has been well-described experimentally.<sup>40,41</sup> While our simulations do not include this specific polymer or reaction, the exothermic formation of gas particles is included and the correlation between the presence of gas molecules, the energy released, and the ensuing ablation can be ascertained.

The MC–MD model allows a tractable PMMA polymer system to be used to study the mechanisms of ablation. Figure 3 displays the computational setup used in the simulations. The system consists of 951 polymer chains with each containing 19 monomer units (109 365 particles) in a 51 Å × 51 Å × 936 Å cell. Periodic boundary conditions are used on the two sides of the sample allowing the simulation of the center of a laser pulse. A pressure-absorbing boundary condition is used at the bottom, which mimics an infinite sample and negates the reflection of a propagating pressure wave in the sample.<sup>37,42</sup> Photons are absorbed exponentially along the depth of the sample according to Beer's law using a penetration depth of 100 Å. Pulse widths of 5 and 150 ps are used in the simulations. A pulse width of 150 ps is within the thermal confinement regime for this sample; that is the thermal energy is deposited in the sample faster than it is able to dissipate by thermal conduction and is confined to the absorbing volume.<sup>43</sup> A pulse width of 5 ps is within the pressure and thermal confinement regimes as the energy is deposited faster than the sample mechanically or thermally relaxes.<sup>43–45</sup> Upon absorption, the photothermal and photochemical channels are modeled in *separate* simulations to *individually* examine different excitations channels and detail their effects on the conditions necessary to achieve ablation.

The simulation parameters described above provide a controlled environment for the examination of several simulation mechanisms. In contrast, a complex set of interconnected

properties of the polymer plays a role in initiating ablation in experiment. For example, at a given wavelength, the precise branching ratios among thermal energy deposition and various photochemical pathways remain elusive. Further complications arise in varying the laser wavelength where the absorption coefficient and, presumably, the branching ratios among the excitation channels change.<sup>9,13,25</sup> The interlinked nature of such experimental factors does not allow for a detailed experimental study of the effects of a one-parameter change on the ablation process. Though parameters such as the experimental absorption coefficients and multiple nanosecond pulses are beyond the scope of MD, the simulations are ideal for studying the separate thermal and chemical mechanisms because the precise microscopic conditions are unknown. Approximations therefore are made to have a reasonable set of parameters (given above), which provides insight into the thermal, chemical, and mechanical aspects of ablation. Additionally, higher quantum yields are used than experimentally observed<sup>13,22</sup> to observe the maximum effects of photochemistry on the ablation process. Because these simulation parameters do not precisely match those used in experiment, an exact quantitative comparison between the results of simulation and experiment is not made. The impact of the thermal and chemical process on the mechanism of ablation though remains valid. Therefore, the hybrid MD technique provides the best tool, and the simulation results allow the best opportunity to qualitatively describe how molecular interactions lead to ablation.

## Excitation Channels and Ablation Mechanisms

The pure photothermal simulations demonstrate the presence of ablation when a critical number of bonds are broken.<sup>43,44</sup> As an example, a simulation using 7.9 eV photons (equivalent to 157 nm radiation), a fluence of 15 mJ/cm<sup>2</sup>, and a pulse width of 150 ps is discussed here. Figure 4 displays four snapshots of the simulation and the corresponding plots of the fraction of particles with thermally broken bonds as a function of depth. In each snapshot, the red and gray beads are

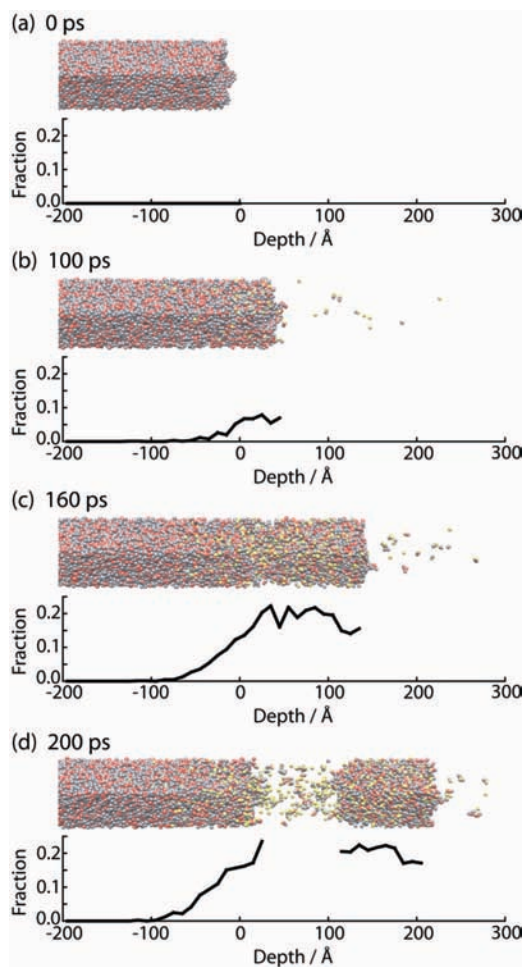


**FIGURE 4.** A series of snapshots of a photothermal simulation using a fluence of  $15 \text{ mJ/cm}^2$ , a penetration depth of  $100 \text{ \AA}$ , and a pulse width of  $150 \text{ ps}$ . The gray and red particles are the original polymer molecules and the yellow particles represent molecules with thermally broken bonds. A plot of the fraction of particles with thermally broken bonds as a function of depth is included with each snapshot. The fraction is only plotted for the bulk material and ejected cluster.

Ⓜ An animation of this simulation in mpg format is available.

particles of the original polymer (see Figure 2) and yellow beads are particles with thermally broken bonds. Initially, there is minimal swelling of the surface of the sample, and particles predominantly evaporate from the surface. By  $100 \text{ ps}$  (Figure 4b), the gradual thermal degradation of the sample is shown as the fraction of particles with broken bonds increases to approximately  $0.10$  and the surface has swelled by  $50 \text{ \AA}$ . In Figure 4c, the continued absorption of photons causes the sample to swell even further by  $160 \text{ ps}$ , and the fraction of particles with broken bonds has increased to nearly  $0.20$ . Ablation is realized by  $200 \text{ ps}$  (Figure 4d) with the ejection of a large cluster of substrate. An animation of the simulation is included as a web-enhanced object. The fraction of particles with broken bonds on the surface of the remaining substrate

and at the bottom of the ejecting cluster is over  $0.20$  and indicates a critical value that is common to all the pure photothermal simulations. In order for ablation to occur for the photothermal simulations, sufficient energy must be deposited in the sample to cause a critical number, in this case  $10\%$ , of the total bonds (corresponding to the  $0.20$  particle fraction) to thermally break. It is important to note that the critical value is specific to the polymer system studied. Longer polymer chains give rise to higher levels of entanglement and would require more thermal decomposition for ablation to occur.<sup>19,20</sup>

In comparison, when photochemistry is introduced into the system, the mechanism of ablation includes chemical decomposition decreasing the connectivity of the sample followed by thermally induced cluster ejection.<sup>43,45,46</sup> Two different channels of photochemistry are investigated for PMMA. In one case, the absorption of a photon leads to the direct scission of the side chain, and a carbon radical on the main chain and a methyl formate radical are formed (Norrish type I reaction). Following this bond cleavage, further chemical reactions produce small molecules such as  $\text{CO}$ ,  $\text{CO}_2$ ,  $\text{CH}_4$ ,  $\text{CH}_3\text{OH}$ , and  $\text{HCOOCH}_3$ , as well as double-bonded carbon on the main chain. In the other case, a photon cleaves the main chain  $\text{C}-\text{CH}_2$  bond (Norrish type II) forming two radicals. Unzipping of the polymer to form MMA can occur, and other chemical reactions eliminate  $\text{CH}_3$  from the main chain, form double-bonded carbon atoms on the main chain, and produce methane. For the discussion of ablation with photochemistry, a Norrish type I simulation is examined using the same photon energy ( $7.9 \text{ eV}$ ), fluence ( $15 \text{ mJ/cm}^2$ ), and pulse width ( $150 \text{ ps}$ ) as the photothermal case. In Figure 5, a series of five snapshots is given showing the time evolution of the simulation along with the plots of density as a function of depth. The same colors designate the original polymer as in the snapshots of Figure 4. The green beads represent various gaseous molecules, the blue beads represent double-bonded carbon atoms, and the yellow beads represent radicals. Two lines are displayed in each density plot corresponding to the total density at a given depth (black) and the contribution of the transformed material (e.g., radicals, gaseous particles, and double-bonded carbon) to the density (red). In this mechanism of ejection, there is rapid formation of gas molecules, which is visible by  $50 \text{ ps}$  (Figure 5b). These gases begin to stream out, and by  $100 \text{ ps}$  (Figure 5c), the sample has been hollowed out such that a small cluster composed of mostly transformed material has ejected. The upper layers of the sample undergo rapid and complete decomposition, and in Figure 5d, ablation sets in as large quantities of this transformed material

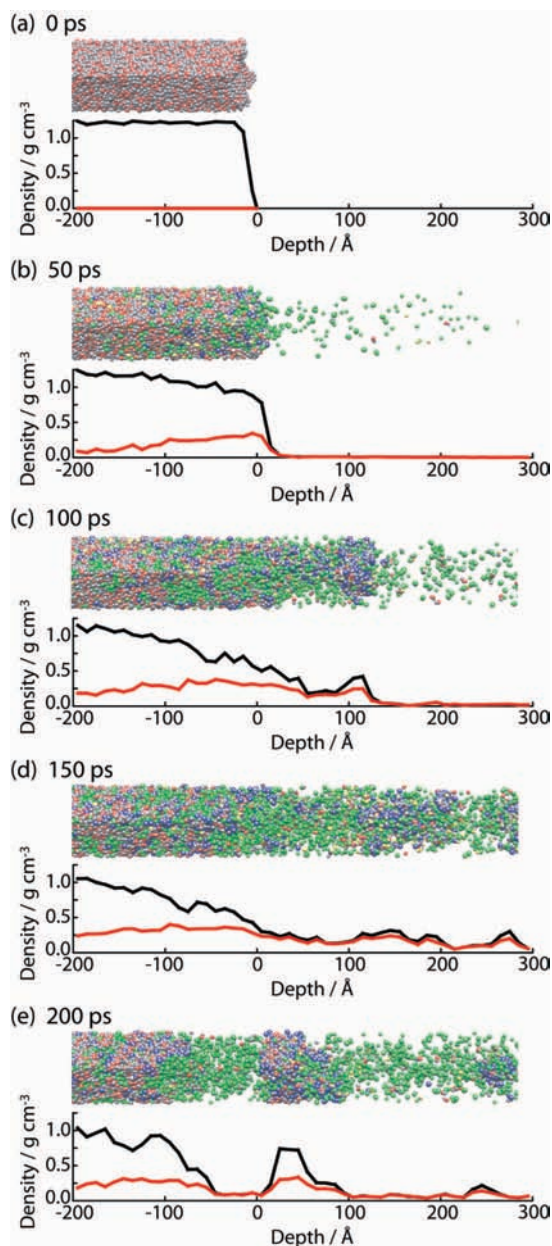


**FIGURE 5.** A series of snapshots of a photochemical simulation with direct side chain cleavage (Norrish type I) and formation of gaseous molecules using a fluence of  $15 \text{ mJ/cm}^2$ , a penetration depth of  $100 \text{ \AA}$ , and a pulse width of  $150 \text{ ps}$ . The gray and red particles are the original polymer molecules, and the yellow, green, and blue particles represent radicals, gas molecules, and double-bonded carbon, respectively. A plot of density as a function of depth is included with each snapshot. The black line is the density of the all the particles, while the red line is the density of the transformed material.

Ⓜ An animation of this simulation in mpg format is available.

eject at  $150 \text{ ps}$ . Eventually, the ejection of a large cluster of substrate is observed at approximately  $200 \text{ ps}$  (Figure 5e) as the transformation of material has decreased the cohesive energy and connectivity between the cluster and the substrate. The ejection of the cluster is thermal in nature, as the gases

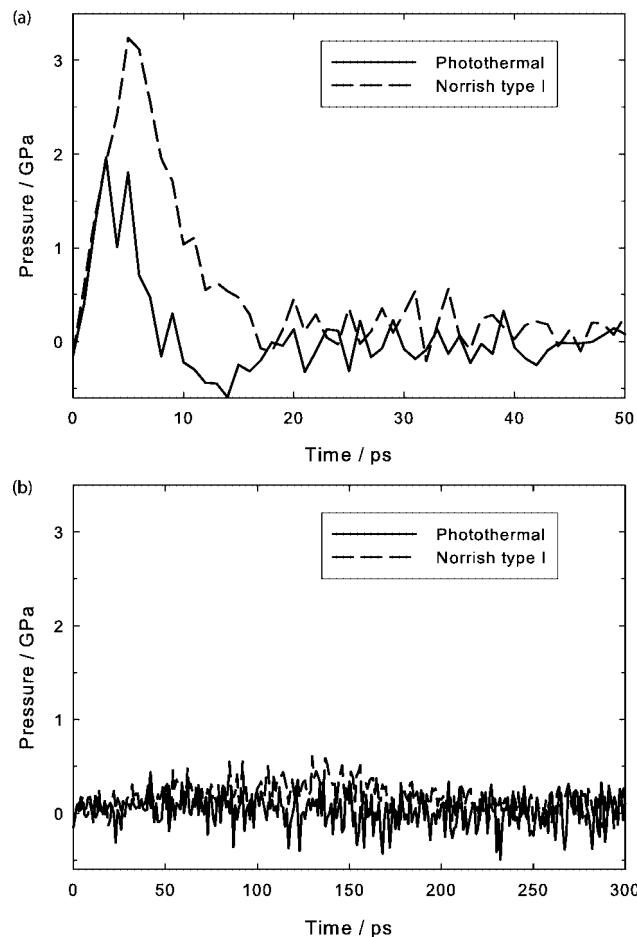


**FIGURE 6.** Pressure at a depth of  $100 \text{ \AA}$  below the surface plotted as a function of time for (a)  $5 \text{ ps}$  pulse width and (b)  $150 \text{ ps}$  pulse width simulations using a fluence of  $15 \text{ mJ/cm}^2$  and a penetration depth of  $100 \text{ \AA}$ . The photothermal simulations are indicated by the solid lines while the Norrish type I photochemical simulations are indicated by the dashed lines.

trapped below do not cause the buildup of high pressure. An animation of this photochemical simulation is included as a web-enhanced object. For the Norrish type II simulations, the mechanism of ablation is similar except the substrate predominantly decomposes into MMA monomer and polymer fragments.

The simulations discussed above illustrate mechanisms where pressure does not contribute to the ejection process. In contrast, MD simulations of molecular solids have shown that when a sufficiently short pulse is used the substrate becomes stress confined, and pressure is a major contributor in causing ablation.<sup>34</sup> Likewise, PMMA simulations using a short pulse show that pressure can play a role in initiating ablation.<sup>43,44</sup> In Figure 6, the pressure profile at a depth of  $100 \text{ \AA}$  below the surface is shown as a function of time for photothermal and photochemical (Norrish type I) simulations using  $7.9 \text{ eV}$  photons, a fluence of  $15 \text{ mJ/cm}^2$ , and pulse

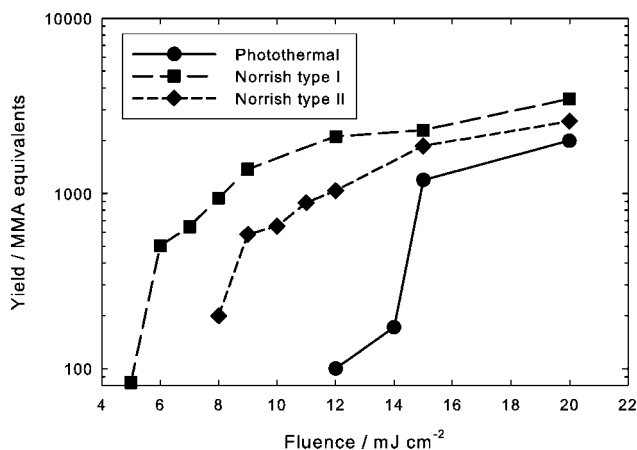


**FIGURE 7.** The yield in MMA equivalents plotted as a function of fluence for the photothermal (●), Norrish type I (■), and Norrish type II (◆) simulations using 7.9 eV photons and a 150 ps pulse width.

widths of 5 ps (a) and 150 ps (b). A pressure wave moving throughout the substrate is apparent with the 5 ps pulse and negligible for the 150 ps pulse. The stress on the system results in a more violent ejection process using the short pulse. For the photothermal case, the propagating compressive pressure wave is followed by a tensile wave, which forms as the pressure wave reflects off the surface. The high stress on the sample (which is greater than the tensile strength of the material) contributes to the fracture of bonds and the resulting high velocity material ejection. In the short pulse photochemical simulation, the rapid deposition of energy causes the formation of the pressure wave, which has a larger magnitude than the compressive pressure wave of the photothermal simulation at the same fluence. This higher pressure is due to the decomposition of the material into gases and small molecules. Additionally, the tensile pressure observed in the photothermal simulation is absent in the photochemical case. The change in the composition of the material from an interconnected, amorphous polymer to gases and small molecules largely prevents the formation of a tensile wave. The pressure effects on ablation in the polymer simulations can be compared with experimental work.<sup>11,47</sup> In the experimental studies, the rapid deposition of heat or formation of photo-products creates an acoustical wave in polymeric materials, which assists in the ejection of material.

## Impact of Photochemistry

A common element in the simulations is that ablation occurs after degradation of material. An examination of the ablation thresholds and the amount of material ejected for the photothermal and photochemical cases reveals the enhancement in ablation due to photochemistry. In Figure 7, the yield mea-

sured in MMA equivalents resulting after excitation is plotted as a function of fluence for the photothermal, the Norrish type I and the Norrish type II simulations using a 7.9 eV photon energy and a pulse width of 150 ps. A dramatic increase in the number of particles ejected (approximately an order of magnitude) demarcates the threshold between the ablation and desorption regions. Observation of large clusters of substrate in the plume also characterizes the ablation regime, while in the desorption regime, small particles (gas molecules and polymer fragments) evaporate from the surface.<sup>34,43</sup> The threshold fluence is realized in the simulations when the amount of ejected material is approximately 800–1000 MMA units. This yield corresponds to the appearance of clusters of substrate within the plume as shown in the snapshots of Figures 4 and 5.

In comparing the photothermal and photochemical results, the excitation channel used significantly affects the ablation threshold and yield. The Norrish type I simulation has the lowest threshold and the largest amount of material ejected, while the photothermal simulation has the highest threshold and the least amount of material ejected. In the Norrish type I set of simulations, photochemical bond cleavages are followed by rapid chemical decomposition of material, and ablation occurs with a comparatively low fluence (fewer number of photons). In contrast, the photons in the photothermal simulations are absorbed as heat and do not directly break bonds. In the absence of chemical reactions, the material maintains its original connectivity, and the amount of energy required to heat the system and mechanically break bonds for ablation is supplied with a higher fluence (greater number of photons). The effect of photochemistry is further illustrated with the Norrish type II simulations where the photons are absorbed both photothermally and photochemically. Since there are direct bond cleavages and further chemical reactions, rapid material breakdown occurs. The photochemical quantum yield, however, is lower than the Norrish type I simulations, which is reflected in the shift in the threshold. An enhancement in the yield with photochemistry can also be observed when lower energy photons are used.<sup>46</sup> Though absorption characteristics differ with changing photon energy, or wavelength,<sup>9</sup> the simulations do not include this change in parameter and only examine the energetic and chemical effects, not quantum yields. If the same penetration depth is used, a greater number of lower energy photons are absorbed by the substrate at a given fluence. More photochemistry and material decomposition occur resulting in a larger yield.

The simulations highlight the effects of photochemistry in the ablation process and are complementary to experimen-

tal studies. The simulations demonstrate that by increasing photochemistry in a polymer system greater decomposition takes place and ablation happens at a lower fluence. While the exact role of such processes in initiating ablation in pure polymers remains a subject of contention, researchers have successfully harnessed the nature of dopants and chromophores to increase photochemical activity and enhance ablation in polymers.<sup>27,41,48–51</sup> Studies of doped PMMA performed by Srinivasan show that the photochemical decomposition of the dopant leads to ablation using a wavelength that PMMA negligibly absorbs.<sup>27</sup> More recently, polymers have been designed to include particular photolabile groups, which readily decompose, release a large amount of energy, and decrease the ablation threshold.<sup>41,48–51</sup>

## Microscopic Physics and Bulk Ablation Models

MD simulations give a detailed description of the underlying mechanisms of ejection and are able to provide microscopic evidence to support macroscopic models of ablation. The issue is whether the microscopic insights connect with the macroscopic models of photothermal and photochemical ablation. For example, Zhigilei and Garrison used an analytic expression to describe the amount of material ejected above the ablation threshold for MD simulations of a molecular solid.<sup>34</sup> In this model, a critical energy density characterizes the amount of energy necessary to initiate ablation in surface layers. For the ablation simulations of PMMA, a critical energy also can define ablation, but the value is affected by the amount of photochemistry.<sup>52</sup> When more photochemistry is introduced into the system, there is a decrease in the energy that must be attained at a given depth to trigger ablation. As described in the preceding section, the Norrish type I simulations have the most photochemistry occurring and result in the lowest critical energy, approximately 3.6 eV/monomer, necessary for ablation. This energy is equivalent to a single carbon–carbon bond per monomer. Since less photochemistry occurs during the Norrish type II simulations, a higher critical energy describes the condition for ablation. The highest critical energy of approximately 7 eV/monomer is required for ablation of the pure photothermal simulations. In that case, the photons do not directly cleave the bonds and chemical reactions in the material do not occur. Consequently, the largest amount of energy is needed.

Further comparisons can be made between the results of the photothermal simulations and analytical models of ablation. The bulk photothermal model given by Bityurin describes ablation in polymers as the systematic removal of material fol-

lowing the thermally induced formation of broken bonds.<sup>53</sup> Ablation is defined when the fraction of material at the surface attains a critical number of broken bonds. We have shown that in the photothermal simulations of PMMA, a critical number of broken bonds is observed before cluster ejection begins. When the evolution of the broken bonds in the simulations is fit to the appropriate part of the analytical model, there is good agreement to the functional form and the numerical values of the parameters.<sup>43</sup> The photothermal simulations therefore substantiate the thermal model of Bityurin.

The ablation mechanisms described by the photochemical simulations also supplement analytical models of polymer ablation. Detailed models of photochemical modification of material are found in the literature.<sup>8,17,54–56</sup> The model of Kalonartov proposes that ablation happens in two steps beginning with the photolytic decomposition of material followed by thermally activated ejection of material.<sup>55</sup> Our simulation data fit well to the model; however, the small molecules are not accounted in our fits because their ejection is not described by this model.<sup>43</sup> As discussed in the previous sections, the formation and ejection of small molecules are important contributors to the ablation process, and a more complete description is warranted.

## Concluding Remarks

Molecular simulation is able to advance the understanding of ablation in polymeric materials by elucidating the microscopic effects of chemistry on the ejection process. The methodology described in this Account allows for various mechanisms of polymer ablation to be studied using a straightforward MC reaction scheme embedded within a MD simulation. From the simulations, the presence of photochemistry is shown to lead to the rapid transformation of the polymer into gas and smaller fragments. With an increasing amount of this type of chemical decomposition, the cohesive energy of the substrate is reduced, less energy is required to initiate ejection, and lower ablation thresholds are observed. Considering the implications of these findings, promoting photochemical reactions in laser-material interactions is advantageous in setting ablation with a minimal amount of input energy. Continued research to advance the understanding of the interplay between photoprocesses and ablation in polymeric materials remains a challenging yet fruitful endeavor.

*This work was supported by the National Science Foundation through the Information Technology and Research Program Grant No. 0426604 and the U.S. Air Force Office of Scientific*



Research through the Multi-University Research Initiative. We would like to thank Yaroslava Yingling, Leonid Zhigilei, R. Srinivasan, and Thomas Lippert for many stimulating discussions on laser ablation.

#### BIOGRAPHICAL INFORMATION

**Patrick Conforti** received his B.S. in chemistry from the University of Notre Dame in 2003. He is currently a Ph.D. candidate at Penn State University where his advisor is Barbara Garrison. His thesis focuses on investigating the mechanisms of ablation in polymers.

**Manish Prasad** graduated from the University of Pennsylvania in 2004 with a Ph.D. in Chemical and Biomolecular Engineering where his advisor was Talid Sinno. He is currently working as a postdoctoral scholar at Penn State University.

**Barbara J. Garrison** received her Ph.D. in 1975 at the University of California at Berkeley, where her mentors were Professors William A. Lester, Jr., William H. Miller, and Henry F. Schaefer, III. After a postdoctoral appointment at Purdue University, she joined the chemistry faculty of Penn State University in 1979. Her group is actively involved in understanding fast energy deposition processes at surfaces. More information can be found at <http://www.chem.psu.edu/faculty/bjg/>.

#### FOOTNOTES

\*To whom correspondence should be addressed. E-mail: [bjg@psu.edu](mailto:bjg@psu.edu).

#### REFERENCES

- Bäuerle, D. *Laser Processing and Chemistry*; Springer-Verlag: Berlin Heidelberg, 2000.
- Gómez, D.; Goenaga, I.; Lizuain, I.; Ozaita, M. Femtosecond laser ablation for microfluidics. *Opt. Eng.* **2005**, *44*, 051105.
- Fardel, R.; Nagel, M.; Nüesch, F.; Lippert, T.; Wokaun, A. Fabrication of organic light-emitting diode pixels by laser-assisted forward transfer. *Appl. Phys. Lett.* **2007**, *91*, 061103/1–061103/3.
- Bituryn, N. Studies on laser ablation of polymers. *Annu. Rep. Prog. Chem., Sect. C, Phys. Chem.* **2005**, *101*, 216–247.
- Krajnovich, D. J. Incubation and photoablation of poly(methyl methacrylate) at 248 nm. New insight into the reaction mechanism using photofragment translational spectroscopy. *J. Phys. Chem. A* **1997**, *101*, 2033–2039.
- Lippert, T. Interaction of photons with polymers: From surface modification to ablation. *Plasma Process. Polym.* **2005**, *2*, 525–546.
- Lippert, T.; Dickinson, J. T. Chemical and spectroscopic aspects of polymer ablation: Special features and novel directions. *Chem. Rev.* **2003**, *103*, 453–485.
- Bituryn, N.; Luk'yanchuk, B. S.; Hong, M. H.; Chong, T. C. Models for laser ablation of polymers. *Chem. Rev.* **2003**, *103*, 519–552.
- Srinivasan, R.; Braren, B.; Casey, K. B. Ultraviolet laser ablation and decomposition of organic materials. *Pure Appl. Chem.* **1990**, *62*, 1581–1584.
- Blanchet, G. B.; Cotts, P.; Fincher, C. R. Incubation: Subthreshold ablation of poly(methyl methacrylate) and the nature of the decomposition pathways. *J. Appl. Phys.* **2000**, *88*, 2975–2978.
- Dyer, P. E.; Srinivasan, R. Nanosecond photoacoustic studies on ultraviolet-laser ablation of organic polymers. *Appl. Phys. Lett.* **1986**, *48*, 445–447.
- Estler, R. C.; Nogar, N. S. Mass spectroscopic identification of wavelength dependent UV laser photoablation fragments from polymethylmethacrylate. *Appl. Phys. Lett.* **1986**, *49*, 1175–1177.
- Küper, S.; Modaressi, S.; Stuke, M. Photofragmentation pathways of a PMMA model compound under UV excimer laser ablation conditions. *J. Phys. Chem.* **1990**, *94*, 7514–7518.
- Küper, S.; Stuke, M. UV-excimer-laser ablation of polymethylmethacrylate at 248 nm - characterization of incubation sites with fourier-transform IR-spectroscopy and UV-spectroscopy. *Appl. Phys. A: Mater. Sci. Process.* **1989**, *49*, 211–215.
- Srinivasan, R.; Braren, B.; Seeger, D. E.; Dreyfus, R. W. Photochemical cleavage of a polymeric solid - details of the ultraviolet-laser ablation of poly(methyl methacrylate) at 193 and 248 nm. *Macromolecules* **1986**, *19*, 916–921.
- Tsunekawa, M.; Nishio, S.; Sato, H. Laser-ablation of polymethylmethacrylate and polystyrene at 308 nm - demonstration of thermal and photothermal mechanisms by a time-of-flight mass spectroscopic study. *J. Appl. Phys.* **1994**, *76*, 5598–5600.
- Srinivasan, R.; Braren, B. Ultraviolet-laser ablation of organic polymers. *Chem. Rev.* **1989**, *89*, 1303–1316.
- Hatanaka, K.; Kawao, M.; Tsuboi, Y.; Fukumura, H.; Masuhara, H. Switching from photochemical to photothermal mechanism in laser ablation of benzene solutions. *J. Appl. Phys.* **1997**, *82*, 5799–5806.
- Bounos, G.; Selimis, A.; Georgiou, S.; Rebillar, E.; Castillejo, M.; Bituryn, N. Dependence of ultraviolet nanosecond laser polymer ablation on polymer molecular weight: Poly(methyl methacrylate) at 248 nm. *J. Appl. Phys.* **2006**, *100*, 114323.
- Rebollar, E.; Bounos, G.; Oujja, M.; Domingo, C.; Georgiou, S.; Castillejo, M. Influence of polymer molecular weight on the chemical modifications induced by UV laser ablation. *J. Phys. Chem. B* **2006**, *110*, 14215–14220.
- Rebollar, E.; Bounos, G.; Oujja, M.; Georgiou, S.; Castillejo, M. Effect of molecular weight on the morphological modifications induced by UV laser ablation of doped polymers. *J. Phys. Chem. B* **2006**, *110*, 16452–16458.
- Fedynshyn, T. H.; Kunz, R. R.; Sinta, R. F.; Goodman, R. B.; Doran, S. P. Polymer photochemistry at advanced optical wavelengths. *J. Vac. Sci. Technol. B* **2000**, *18*, 3332–3339.
- Cozzens, R. F.; Fox, R. B. Infrared laser ablation of polymers. *Polym. Eng. Sci.* **1978**, *18*, 900–904.
- Srinivasan, R. Ablation of polyimide (Kapton) films by pulsed (ns) ultraviolet and infrared (9.17  $\mu\text{m}$ ) lasers. *Appl. Phys. A: Mater. Sci. Process.* **1993**, *56*, 417–423.
- Srinivasan, R. Ablation of polymethyl methacrylate films by pulsed (ns) ultraviolet and infrared (9.17  $\mu\text{m}$ ) lasers: A comparative study by ultrafast imaging. *J. Appl. Phys.* **1993**, *73*, 2743–2750.
- Lippert, T.; Webb, R. L.; Langford, S. C.; Dickinson, J. T. Dopant induced ablation of poly(methyl methacrylate) at 308 nm. *J. Appl. Phys.* **1999**, *85*, 1838–1847.
- Srinivasan, R.; Braren, B. Ultraviolet laser ablation and etching of polymethyl methacrylate sensitized with an organic dopant. *Appl. Phys. A: Mater. Sci. Process.* **1988**, *45*, 289–292.
- Allen, M. P.; Tildesley, D. J. *Computer Simulations of Liquids*; Oxford University Press: Oxford, 1987.
- Dou, Y. S.; Zhigilei, L. V.; Winograd, N.; Garrison, B. J. Explosive boiling of water films adjacent to heated surfaces: A microscopic description. *J. Phys. Chem. A* **2001**, *105*, 2748–2755.
- Dutkiewicz, L.; Johnson, R. E.; Vertes, A.; Pedrys, R. Molecular dynamics study of vibrational excitation dynamics and desorption in solid O<sub>2</sub>. *J. Phys. Chem. A* **1999**, *103*, 2925–2933.
- Wu, X. W.; Sadeghi, M.; Vertes, A. Molecular dynamics of matrix-assisted laser desorption of leucine enkephalin guest molecules from nicotinic acid host crystal. *J. Phys. Chem. B* **1998**, *102*, 4770–4778.
- Zhigilei, L. V.; Kodali, P. B. S.; Garrison, B. J. Molecular dynamics model for laser ablation and desorption of organic solids. *J. Phys. Chem. B* **1997**, *101*, 2028–2037.
- Zhigilei, L. V.; Kodali, P. B. S.; Garrison, B. J. A microscopic view of laser ablation. *J. Phys. Chem. B* **1998**, *102*, 2845–2853.
- Zhigilei, L. V.; Garrison, B. J. Microscopic mechanisms of laser ablation of organic solids in the thermal and stress confinement irradiation regimes. *J. Appl. Phys.* **2000**, *88*, 1281–1298.
- Yingling, Y. G.; Garrison, B. J. Photochemical ablation of organic solids. *Nucl. Instrum. Methods Phys. Res., Sect. B* **2003**, *202*, 188–194.
- Yingling, Y. G.; Garrison, B. J. Course-grained chemical reaction model. *J. Phys. Chem. B* **2004**, *108*, 1815–1821.
- Prasad, M.; Conforti, P. F.; Garrison, B. J. Coupled molecular dynamics - Monte Carlo model to study the role of chemical processes during laser ablation of polymeric materials. *J. Chem. Phys.* **2007**, *127*, 084705.
- Lade, R. J.; Morley, I. W.; May, P. W.; Rosser, K. N.; Ashfold, M. N. R. ArF (193 nm) laser ablation of poly(methyl methacrylate). *Diamond Relat. Mater.* **1999**, *8*, 1654–1658.
- Conforti, P. F.; Garrison, B. J. Electronic structure calculations of radical reactions for poly(methyl methacrylate) degradation. *Chem. Phys. Lett.* **2005**, *406*, 294–299.
- Stebani, J.; Nuyken, O.; Lippert, T.; Wokaun, A. Synthesis and characterization of a novel photosensitive triazene polymer. *Makromol. Chem. Rapid Commun.* **1993**, *14*, 365–369.
- Lippert, T.; Dickinson, J. T.; Langford, S. C.; Furutani, H.; Fukumura, H.; Masuhara, H.; Kunz, T.; Wokaun, A. Photopolymers designed for laser ablation - photochemical ablation mechanism. *Appl. Surf. Sci.* **1998**, *129*, 117–121.

- 42 Zhigilei, L. V.; Garrison, B. J. Pressure waves in microscopic simulations of laser ablation. *Mater. Res. Soc. Symp. Proc.* **1999**, *538*, 491–496.
- 43 Prasad, M.; Conforti, P. F.; Garrison, B. J. On the role of chemical reactions initiating UV ablation in poly(methyl methacrylate). *J. Appl. Phys.* **2007**, *101*, 103113.
- 44 Conforti, P. F.; Prasad, M.; Garrison, B. J. Effects of thermal energy deposition on material ejection in poly(methyl methacrylate). *Appl. Surf. Sci.* **2007**, *253*, 6386–6389.
- 45 Prasad, M.; Conforti, P. F.; Garrison, B. J.; Yingling, Y. G. Computational investigation into the mechanisms of UV ablation of poly (methyl methacrylate). *Appl. Surf. Sci.* **2007**, *253*, 6382–6385.
- 46 Conforti, P. F.; Prasad, M.; Garrison, B. J. Simulations of laser ablation of poly(methyl methacrylate): Fluence versus number of photons. *J. Phys. Chem. C* **2007**, *111*, 12024–12030.
- 47 Srinivasan, R.; Kelly, G. C.; Bodil, B.; Mildred, Y. The significance of a fluence threshold for ultraviolet laser ablation and etching of polymers. *J. Appl. Phys.* **1990**, *67*, 1604–1606.
- 48 Srinivasan, R.; Braren, B.; Dreyfus, R. W.; Hadel, L.; Seeger, D. E. Mechanism of the ultraviolet laser ablation of polymethyl methacrylate at 193 and 248 nm: Laser-induced fluorescence analysis, chemical analysis, and doping studies. *J. Opt. Soc. Am. B: Opt. Phys.* **1986**, *3*, 785–791.
- 49 Wen, X.; Hare, D. E.; Dlott, D. D. Laser ablation threshold lowered by nanometer hot spots. *Appl. Phys. Lett.* **1994**, *64*, 184–186.
- 50 Lippert, T.; Dickinson, J. T.; Hauer, M.; Kopitkovas, G.; Langford, S. C.; Masuhara, H.; Nuyken, O.; Robert, J.; Salmio, H.; Tada, T.; Tomita, K.; Wokaun, A. Polymers designed for laser ablation-influence of photochemical properties. *Appl. Surf. Sci.* **2002**, *197*, 746–756.
- 51 Lippert, T.; Hauer, M.; Phipps, C.; Wokaun, A. Polymers designed for laser applications- fundamentals and applications. *Proc. SPIE-Int. Soc. Opt. Eng.* **2002**, *4760*, 63–71.
- 52 Conforti, P. F.; Prasad, M.; Garrison, B. J. On the correlation between the photoexcitation pathways and the critical energies required for ablation of poly(methyl methacrylate): A molecular dynamics study. *J. Appl. Phys.* **2008**, *103*, 103–114.
- 53 Bityurin, N.; Malyshev, A. Bulk photothermal model for laser ablation of polymers by nanosecond and subpicosecond pulses. *J. Appl. Phys.* **2002**, *92*, 605–613.
- 54 Johnson, R. E. In *Large Ions: Their Vaporization, Detection and Structural Analysis*; Baer, T., Ng, C. Y., Powis, I., Eds.; John Wiley: New York, 1996; pp 49.
- 55 Kalontarov, L. I.; Marupov, R. Laser-induced polymer ablation: Photochemical decay plus thermal desorption. *Chem. Phys. Lett.* **1992**, *196*, 15–20.
- 56 Luk'yanchuk, B.; Bityurin, N.; Anisimov, S.; Bauerle, D. The role of excited species in UV-laser materials ablation I. Photophysical ablation of organic polymers. *Appl. Phys. A: Mater. Sci. Process.* **1993**, *57*, 367–374.